



## COMPARATIVE PROPERTIES OF CHITOSAN HYDROCHLORIDE AND CHITOSAN NANOACETATE FROM *BOMBYX MORI*

Pirniyazov K.K., Rashidova S.Sh.

*Institute of Polymer Chemistry and Physics Uzbekistan Academy of Sciences, 100128, Tashkent, Uzbekistan*

ARTICLE INFO	ABSTRACT
<p>Received: 04 September 2025 Revised: 02 October 2025 Accepted: 07 October 2025</p> <p><b>Keywords:</b> hydrochloride chitosan Bombyx mori, nanoacetate chitosan Bombyx mori, degree of binding, nanoparticle size, IR spectroscopy, UV spectroscopy</p> <p><b>Corresponding author:</b> Pirniyazov K.K. <a href="mailto:qudratpirniyazov8875@gmail.com">qudratpirniyazov8875@gmail.com</a></p>	<p>The synthesis of chitosan nanoderivatives with various acids in the presence of sodium tripolyphosphate stabilizer was carried out using the ionotropic gelation method. The effects of the component ratios of chitosan and hydrochloric and acetic acids on the formation of hydrochloride chitosan and nanoacetate chitosan from Bombyx mori were evaluated. Structural and physicochemical characteristics of hydrochloride chitosan and nanoacetate chitosan were determined using Atomic Force Microscopy (AFM), X-ray Diffraction Analysis (XRD), Infrared (IR), and Ultraviolet (UV) spectroscopy.</p>

### Introduction

Chitosan (CS) possesses growth-regulating and antimicrobial properties. To enhance its growth-stimulating and antifungal effects, water-soluble complexes of chitosan with certain organic acids such as ascorbic, citric, acetic, and hydrochloric acids are used [1–3]. Complexes chitosan with hydrochloric acid (HCA) play a multifunctional role in the development of agricultural crops and exhibit biological activity against bacteria [4–5]. Currently, there are many chitosan derivative-based products available commercially as plant growth stimulators in agriculture. For example, chitosan hydrochloride (CSHC) exhibits fungicidal, bactericidal, and elicitor properties in protecting agricultural crops from diseases [5].

The use of new economically efficient and environmentally safe alternative chitosan derivatives with hydrochloric acid in agriculture contributes to the reduction of synthetic pesticide application. In study [5], an *in vitro* investigation was conducted to evaluate the antimicrobial and antioxidant activity of chitosan hydrochloride (CSHC) at concentrations of 1 %, 0.5 %, 0.25 %, 0.1 %, 0.05 %, and 0.025 %. As a result, the mycelial growth of *M. laxa* and *M. fructigena* was completely inhibited at HCCS concentrations of 1–0.25 %, while *M. fructicola* was inhibited at concentrations of 1–0.5 %. At a CSHC concentration of 0.25 %, inhibition was observed for *M. fructicola*, *A. brassicicola*, *A. alternata*, and *B. cinerea*, with inhibition zones of 93.99 %, 80.99 %, 69.73 %, and 57.23 %, respectively.

The obtained results on antimicrobial activity indicate the potential for using chitosan hydrochloride (CSHC) as a substitute for imported products and synthetic pesticides. It is well known that synthetic pesticides, including fungicides, accumulate in the soil and pose a risk to the health of animals and humans. In this regard, the application of chitosan hydrochloride against

*Fusarium graminearum* has been shown to enhance germination rate, root development, and improve the nitrogen balance index in durum wheat [6].

In study [7], the high efficacy and safety of the natural derivative chitosan hydrochloride under *in vitro* and *in vivo* conditions were described. Its effectiveness against the *Phytophthora infestans* culture was evaluated, revealing that a CSHC concentration of 0.2–0.4 % was optimal, with an efficacy of 99.3 % under natural conditions. This result enables the broader use of chitosan derivatives as safe substances that can reduce the pesticide load on the soil [7].

The significant antifungal potential of chitosan hydrochloride was demonstrated in study [8], where excellent inhibitory effects were achieved against fungi from pathogenic and toxigenic groups such as *Aspergillus*, *Fusarium*, and *Penicillium*. This is mainly attributed to the complex biology of these pathogens, as well as their various infectious stages during pathogenesis. The initial phase of tissue invasion and destruction typically occurs rapidly, accompanied by the release of motile flagellated zoospores [9–10]. Some studies mention a more likely indirect secondary effect of chitosan applied to plants, such as enhanced plant resistance through the activation of defense mechanisms in the tissue, as well as the mechanical barrier formed by the polymer layer of chitosan hydrochloride [10–11].

Water-soluble forms of chitosan hydrochloride and its low-molecular-weight derivatives are obtained by hydrolyzing high-molecular-weight chitosan in a 1 M hydrochloric acid solution at 70 °C for 4 to 24 hours. The final products are precipitated using ethanol and dried under vacuum, in accordance with the methods described by Inesa V.B. et al. [12, 13].

Overall, the review of the literature does not provide a clear understanding, as the influence of the ratio of chitosan and hydrochloric acid components, as well as the concentration of these components on the properties of the resulting chitosan hydrochlorides, has been insufficiently studied. Therefore, the literature analysis revealed that the effect of synthesis conditions on the complexation of chitosan with hydrochloric acid remains inadequately explored [5, 6, 12, 13].

The reduction in the use of plastic materials has become a significant impetus for the search for biologically active alternatives. Currently, synthetic materials and cellulose-based materials are used as packaging materials. Moreover, these materials degrade poorly and persist in the environment for a long time. In this regard, chitosan has proven to be one of the best materials among such biopolymers. Chitosan acetate films were compared with films produced by conventional methods for packaging purposes. The films based on synthetic polymers showed moderate barrier properties, while the chitosan acetate films demonstrated high barrier performance [14]. Chitosan acetate and nanoacetate were obtained by the methods of sublimation and ionotropic gelation. In the sublimation method, a chitosan solution in 2 % citric acid or 2.0 % acetic acid was frozen at –27 °C for an extended period and then lyophilized for three days to produce microporous films for packaging materials. To obtain chitosan acetate nanoparticles, a 0.5 % chitosan solution in 1–2 % acetic acid with varying pH was titrated with a sodium tripolyphosphate solution at concentrations of 0.25–0.5 % [15, 16].

It should be noted that the literature does not specify the influence of the acetic acid ratio on the formation of chitosan acetate nanoparticles. In many experiments, a 0.5–2% acetic acid solution is used as a solvent without considering the effect of component ratios on the formation of chitosan acetate nanoparticles.

The aim of the present work is the synthesis and investigation of the structural properties of chitosan hydrochloride and chitosan nanoacetate from *Bombyx mori* using XRD, AFM, IR, UV spectroscopy methods, and the determination of their antimicrobial properties.

### Methodology

In this study, chitosan (CS) from *Bombyx mori* (B.M.) with a molecular weight of 98 kDa and a degree of deacetylation (DDA) of 84% was used, obtained from silkworm pupae. The degree of deacetylation (DDA) of the initial chitosan was determined by the conductometric titration method in a 0.1 N hydrochloric acid solvent using a *Mettler Toledo* instrument. In the synthesis of chitosan

hydrochloride, the amount of chitosan was fixed at 0.5 g for all ratios, while the volume of 0.1 N hydrochloric acid was varied between 30 and 7.5 ml according to the component ratio. Chitosan hydrochloride was obtained by mixing deprotonated chitosan and 0.1 N hydrochloric acid in an aqueous solution while varying the ratios of the initial components and the pH of the solution. The reaction to form chitosan hydrochloride was carried out at 25 °C, with a synthesis duration of 60 minutes. Acetone (analytical grade) was used as the precipitant. The amount of hydrochloric acid in the chitosan hydrochloride was determined by alkaline titration in the presence of phenolphthalein indicator. The degree of hydrochloric acid binding was calculated based on the ratio of ( $M_{HCl}$ ) experimental to ( $M_{HC}$ ) theoretical.

**The synthesis of chitosan nanoacetate was carried out using the ionotropic gelation method by varying the ratio of chitosan and acetic acid components.** For the synthesis of chitosan nanoacetate, **chitosan from *Bombyx mori* with a molecular weight of 98 kDa and a degree of deacetylation of 84%** was used. To prepare a 0.05 M solution of acetic acid, **a 92% concentrated solution of acetic acid** was used. In the synthesis of chitosan nanoacetate, a constant amount of 0.5 g of chitosan was used for all component ratios, while the volume of 0.05 M acetic acid solution varied between 60 and 15 mL depending on the component ratio. The reaction was carried out at a temperature of **25°C**, and the synthesis duration was **60 minutes**. **A 0.5% aqueous solution of sodium tripolyphosphate** was used as a stabilizer and cross-linking agent. In the synthesis of chitosan nanoacetate, 110 mL of a 0.5% aqueous solution of sodium tripolyphosphate was used as a stabilizer. The resulting products were dried using **lyophilization (on an Alpha Christ device) at -48°C**.

IR spectra were obtained using an “Inventio-S” FTIR spectrometer (“Bruker”, Germany) in the range of 500 to 4000  $\text{cm}^{-1}$ . X-ray diffraction (XRD) analysis of chitosan and its derivatives was carried out using a *Miniflex 600* X-ray diffractometer (“Rigaku”, Japan) with monochromatic  $\text{CuK}\alpha$ -radiation (wavelength  $\lambda = 1.5418 \text{ \AA}$ ), at 40 kV and a current of 15 mA.

The samples were analyzed in powder form. Scanning was performed in the  $2\theta$  range from  $2^\circ$  to  $70^\circ$ . UV spectroscopy was conducted using a *Specord 210* spectrophotometer with the following settings: spectral range 190–500 nm, slit width 1 nm, and scan rate 2 nm/s. Sample solutions were prepared in 2% acetic acid.

To compare the antimicrobial properties of chitosan nanoacetate, the inhibition zone of *Fusarium oxysporum* culture growth was determined in Petri dishes, cultivated on agar medium for 48 and 72 hours in a thermostat at 25 °C. The experiments were conducted in duplicate. To determine the average antimicrobial properties of the initial components and chitosan nanoacetate samples, the experiments were carried out in four replicates. The Mean (average value) was calculated using Formula (1):

$$\text{Mean} = \frac{\sum X}{n} \quad [1]$$

where:

$\sum X$  — the sum of all measured values

$n$  — the number of measurements

The Standard Deviation (SD) was evaluated using Formula (2):

$$SD = \sqrt{\frac{\sum (X - \text{Mean})^2}{n - 1}} \quad [2]$$

where:

$X$  — each individual value

Mean — the average (mean) value

SD — represents the dispersion of the data around the mean.

## Results and Discussion

The obtained results confirm that increasing the chitosan ratio in the reaction systems enhances the degree of hydrochloric acid binding and the yield of the final products. It should be noted that the highest degree of acid binding was observed at a component ratio of 3:1. Further increases in chitosan concentration relative to hydrochloric acid lead to only slight changes in the binding degree, solution pH, and product yield. This indicates that at a chitosan-to-hydrochloric acid ratio of 3:1, a high level of saturation of chitosan's amino groups occurs through donor–acceptor interactions with hydrochloric acid. The results are presented in Table 1.

**Table 1**

*Dependence of HCl binding degree during the formation of chitosan hydrochloride on chitosan concentration ( $t = 30^\circ\text{C}$ ,  $\tau = 60$  minutes). HCl concentration = 0.05 mol/L*

Chitosan concentration, mol/L	HCl concentration, $\Delta C$ , mol/L	DB*, %	Reaction pH	Cl content in CSHC, %	Yield, %
0,05	0,021	41,0	1,90	8,02	78,0
0,10	0,032	64,0	4,95	7,48	84,2
0,15	0,040	79,0	5,90	6,01	88,5
0,20	0,038	76,0	6,10	4,15	89,6

\*Degree of HCl binding

To study the structural properties of chitosan hydrochloride, ultraviolet (UV) spectroscopy was used. The spectra of chitosan hydrochloride show absorptions associated with  $n \rightarrow \pi^*$  electronic transitions at wavelengths of 220 and 350 nm. These electronic transitions may occur due to unpaired electrons in the nitrogen amino groups and electrons in the double bonds of the acetamide groups. In the UV spectra of chitosan hydrochloride, with an increasing ratio of hydrochloric acid, a hyperchromic increase in absorption intensity around 240 nm is observed compared to the initial chitosan spectrum, along with a bathochromic shift. This can be explained by the interaction of the unpaired electron pairs of the amino groups in chitosan with hydrochloric acid (Fig. 1).

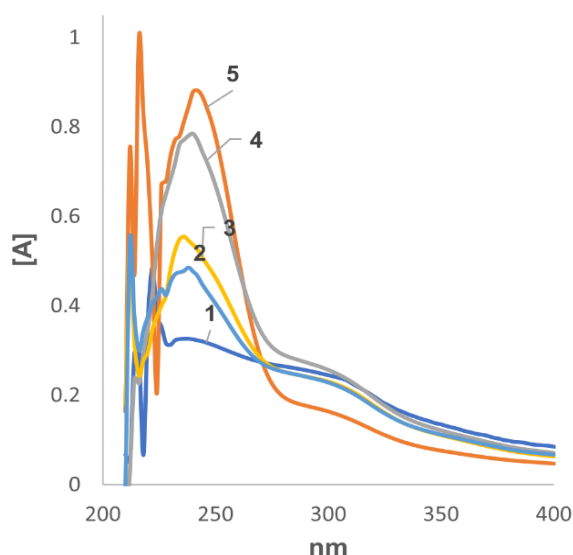


**Figure 1.** UV spectra of samples: 1. Initial chitosan; 2. Chitosan:HCl at a ratio of 4:1; 3. Chitosan:HCl at a ratio of 3:1; 4. Chitosan:HCl at a ratio of 2:1; 5. Chitosan:HCl at a ratio of 1:1.

The structural properties of the initial chitosan were studied using IR spectroscopy. The obtained results show that the IR spectra of chitosan exhibit characteristic absorption bands for acetamide, amino, and methylene groups at 1656, 1600  $\text{cm}^{-1}$ , and 1420  $\text{cm}^{-1}$ , respectively. Additionally, absorption bands corresponding to hydroxyl groups were observed in the 3000–3400  $\text{cm}^{-1}$  region, which is in full agreement with the literature data [13]. In the IR spectra of the obtained chitosan hydrochloride samples, a shift of the absorption bands characteristic of amino groups from 1600 to 1521  $\text{cm}^{-1}$  was detected. This may indicate the formation of a donor–acceptor bond

involving the amino groups of the initial chitosan and the proton of hydrochloric acid. The other absorption bands of chitosan hydrochloride correspond to the IR spectra of the initial chitosan. The results are presented in Figure 2.

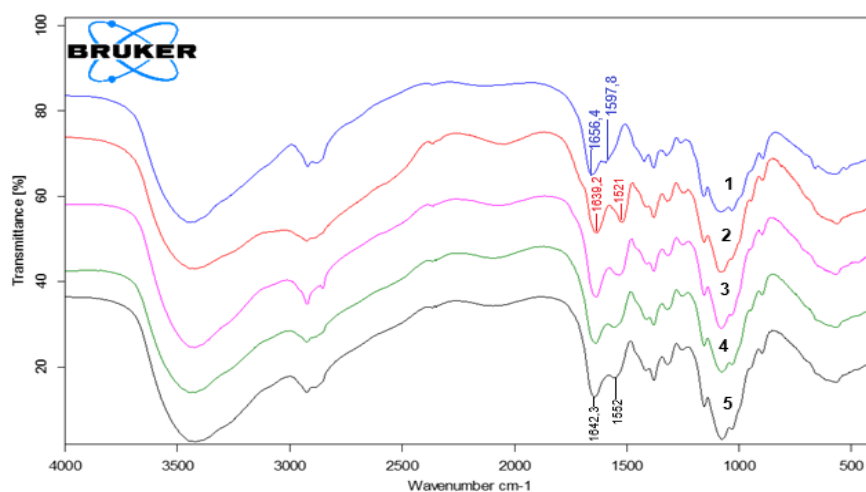


**Figure 2.** IR spectra of chitosan *Bombyx mori* (1), chitosan hydrochloride at component ratios of Chitosan: HCl – 1:1 (2), 2:1 (3), 3:1 (4), and 4:1 (5).

To compare the structural properties of chitosan complexes with organic acids, X-ray structural studies of chitosan hydrochloride were conducted at chitosan-to-hydrochloric acid ratios of 1:1 and 4:1. For the initial chitosan, characteristic diffraction peaks of the chitosan *Bombyx mori* crystalline structure were observed at  $2\theta \approx 10.3^\circ$ ,  $19.9^\circ$ , and  $26.6^\circ$ , corresponding to the interplanar spacings (001), (10-1), and (10-2), respectively. Upon formation of chitosan hydrochloride, a decrease in the intensity of diffraction peaks was observed with an increasing hydrochloric acid content in the complex.

A similar phenomenon is also observed in other chitosan complexes with organic acids. This may be related to the loss of chitosan crystallinity due to interaction with hydrochloric acid, leading to the formation of an amorphous structure. Nevertheless, slight shifts of the peaks toward higher angles were recorded, which is likely associated with a decrease in interplanar distances within the polymer lattice. For example, in the series: acetic acid  $\rightarrow$  ascorbic acid  $\rightarrow$  citric acid  $\rightarrow$  hydrochloric acid, as the acid dissociation constant increases, a transition in the crystal system of the polymer's unit cell occurs from monoclinic to tetragonal. The obtained results are presented in Table 2 and Figure 3.

**Table 2**

*XRD results of chitosan hydrochloride samples*

XRD results of chitosan hydrochloride 1:1			XRD results of chitosan hydrochloride 4:1		
$2\theta, ^\circ$	$d, \text{\AA}$	$a \neq b \neq c$ and $\alpha, \beta, \gamma = 90^\circ$ orthorhombic crystal system	$2\theta, ^\circ$	$d, \text{\AA}$	$a = b \neq c$ and $\alpha, \beta, \gamma = 90^\circ$ tetragonal crystal system
11,9	7,42	020	12,1	6,3	101
19,0	4,60	101	19,2	4,26	102
24,8	3,52	031	21,0	3,39	121

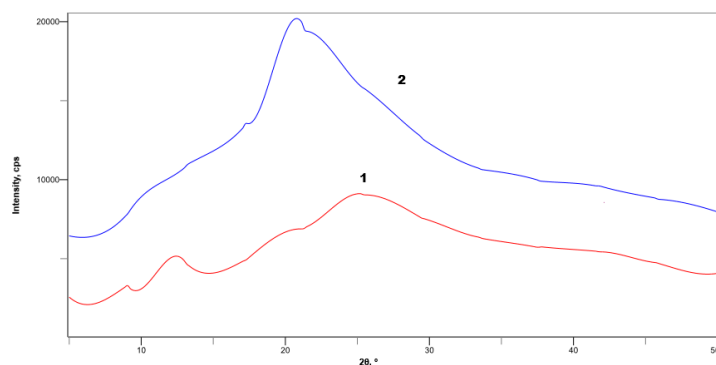


**Figure 3.** XRD results of chitosan hydrochloride at component ratios of 1:1 (curve 1) and 4:1 (curve 2)

The results confirm that with an increase in the hydrochloric acid content in chitosan hydrochloride, an orthorhombic crystal system is established with varying unit cell parameters  $a$ ,  $b$ , and  $c$ . Additionally, with an increase in the chitosan ratio, a tetragonal structure is formed.

The results also confirm that increasing the acetic acid ratio in the reaction systems raises the acetic acid content in chitosan nanoacetate from 7.5% to 22.7%. Compared to hydrochloric acid, the molecular weight of acetic acid is 1.64 times higher, which explains why the acetic acid content is somewhat higher in chitosan nanoacetate compared to chitosan hydrochloride.

It should be noted that during the formation of chitosan nanoacetate, the effect of component ratios differs from the reactions forming chitosan hydrochloride, nanocitrate, and nanoascorbate.

For example, at an equivalent component ratio of chitosan to acetic acid of 1:1:0.5, titration with a sodium tripolyphosphate solution establishes a neutral pH of 7.4, which makes the amino groups of the chitosan macromolecules more reactive. The difference in the pH of the reaction systems depends on the acid dissociation constant. For instance, the dissociation constant for acetic acid is  $K_a = 1.74 \times 10^{-5}$ . For comparison, the dissociation constants for ascorbic acid and hydrochloric acid are  $K_{a1} = 9.12 \times 10^{-5}$  and  $K_a = 1 \times 10^7$ , respectively. This means that hydrochloric acid is stronger compared to acetic, citric, and ascorbic acids.

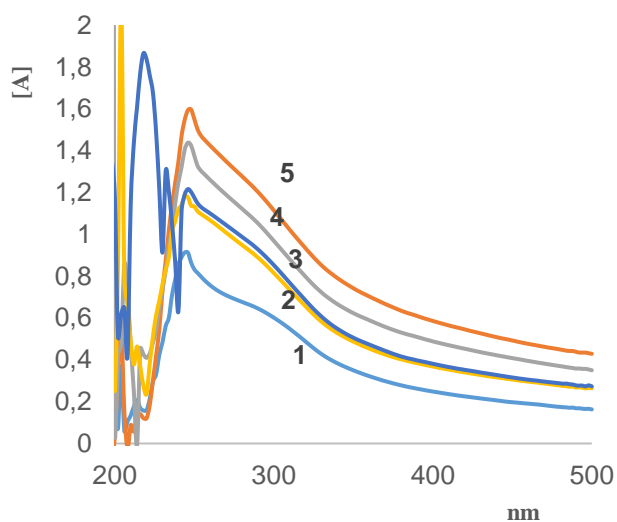
Therefore, under the same conditions, during the formation of chitosan hydrochloride, a pH of 1.9 is established. Furthermore, under identical conditions, increasing the chitosan ratio (at component ratios of 3:1:0.5 and 4:1:0.5) results in only slight changes in the yield of the final products and the solution pH, which may indicate the influence of the weakly alkaline pH of the reaction system. The obtained results are presented in Table 3.

**Table 3**

*Dependence of acetic acid binding degree during the formation of chitosan nanoacetate on chitosan concentration ( $t = 30^\circ\text{C}$ ,  $\tau = 60 \text{ min.}$ ). Acetic acid concentration 0.05 mol/L*

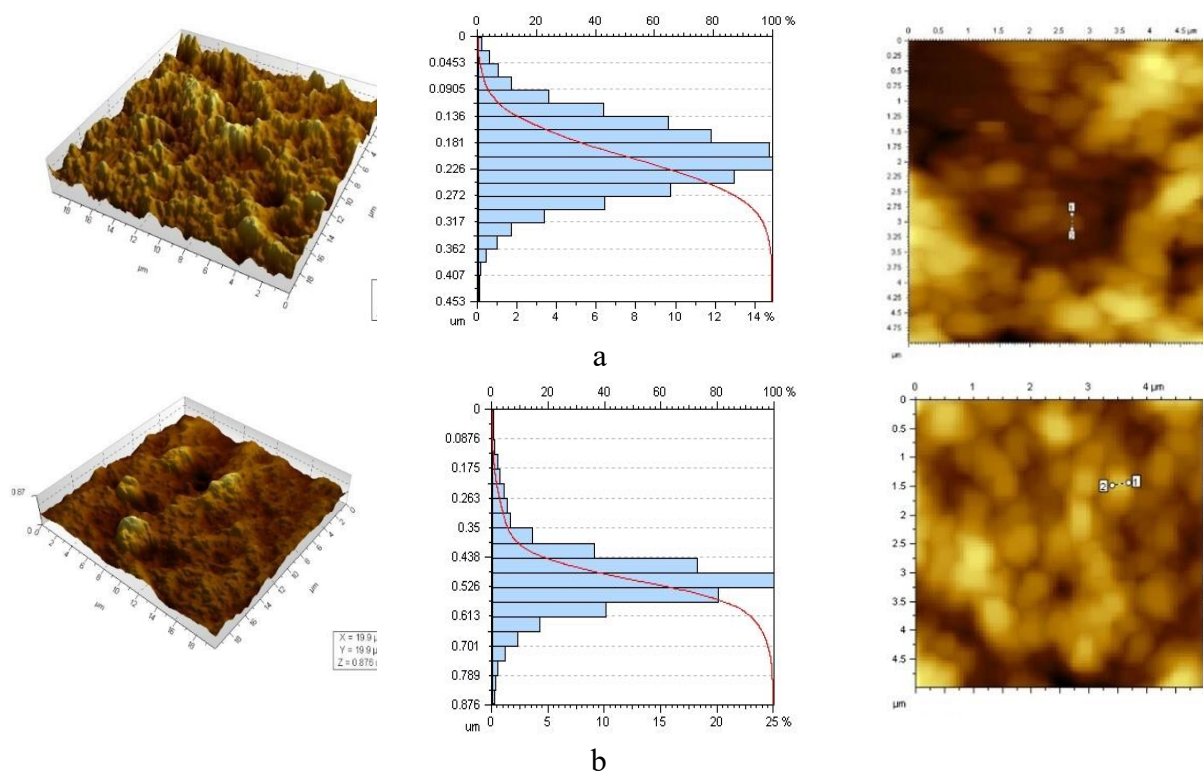
Chitosan concentration, mol/L	$\Delta C_{\text{CH}_3\text{COOH}}$ mol/L	DB, %	Reaction pH	$\text{CH}_3\text{COOH}$ content %	N, %	Yield, %
0,05	0,043	86,0	7,40	22,7	3,96	82,1
0,10	0,040	81,5	8,02	12,4	4,78	84,6
0,15	0,042	83,9	8,44	8,9	5,19	90,7
0,20	0,045	89,2	8,50	7,5	5,44	89,3

The UV spectra of chitosan nanoacetate exhibit similar characteristics compared to the UV-spectrum of chitosan hydrochloride. In both cases, increasing the acid component ratio leads to a hyperchromic increase in the intensity of the absorption band, as well as a bathochromic shift of the absorption band associated with  $n \rightarrow \pi^*$  electronic transitions at wavelengths of 220 and 300 nm. These electronic transitions may occur due to unpaired electrons in the nitrogen amino groups and the electrons of the double bond in the carboxyl groups of acetic acid (Fig. 4).



**Figure 4.** UV spectra of the samples: 1. Initial CS; 2. CS:CH<sub>3</sub>COOH at a ratio of 4:1; 3. CS:CH<sub>3</sub>COOH at a ratio of 3:1; 4. CS:CH<sub>3</sub>COOH at a ratio of 2:1; 5. CS:CH<sub>3</sub>COOH at a ratio of 1:1.

Atomic force microscopy (AFM) results confirm that in the obtained chitosan nanoacetate samples at a component ratio of chitosan: acetic acid: NaTPP = 1:1:0.5, nanoparticles ranging in size from 50 to 300 nm are formed with uniform surface distribution. Additionally, with an increase in the chitosan ratio, the particle size increases to approximately 400–500 nm (Fig. 5).



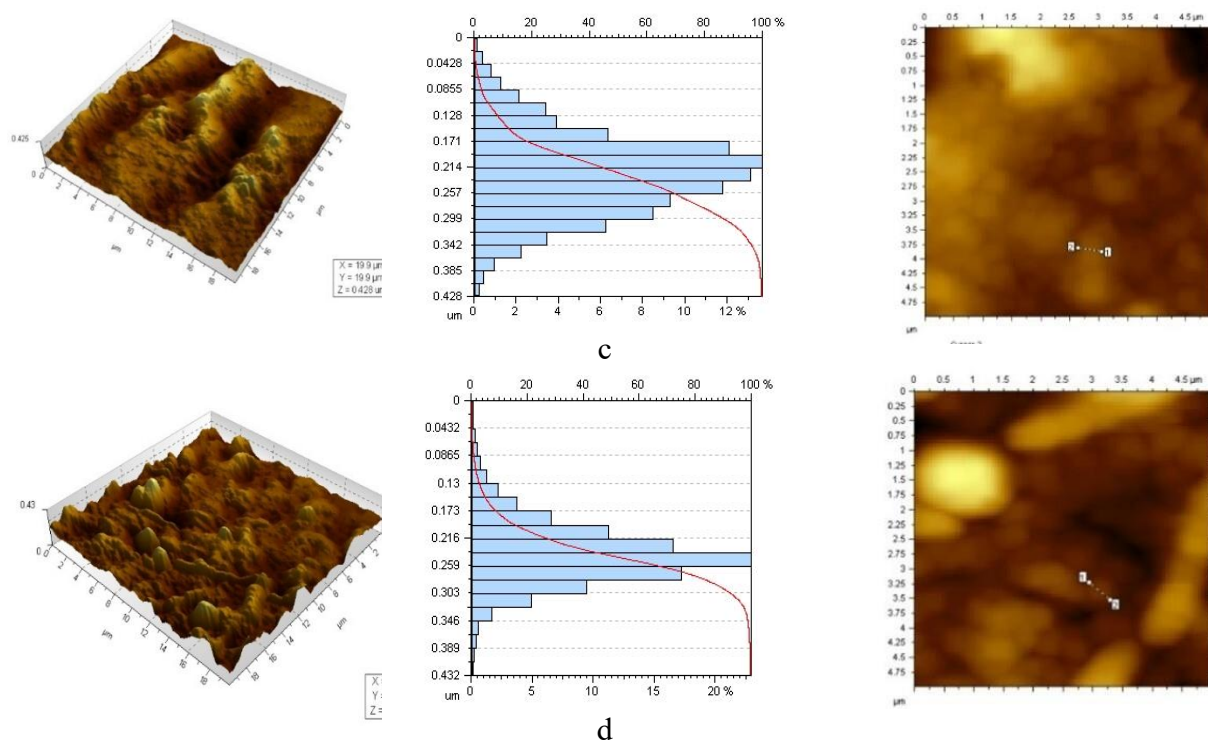


**Figure 5.** Surface topography of chitosan nanoacetate nanoparticles at component ratios of CS:CH<sub>3</sub>COOH:NaTPP — 1:1:0.5 (a); 2:1:0.5 (b); 3:1:0.5 (c); 4:1:0.5 (d)

In the IR spectra of the obtained chitosan nanoacetate samples, a new absorption band was observed in the region of 1530 cm<sup>-1</sup>, indicating the formation of a donor–acceptor bond involving the amino groups of the initial chitosan and the acetate ions of acetic acid. These absorption bands are not present in the IR spectrum of the initial chitosan. Moreover, as the proportion of acetic acid in the chitosan nanoacetate increases, the intensity of the absorption band in the 1530–1520 cm<sup>-1</sup> region also increases. Thus, the formation of nanoparticles complexes of chitosan with organic acids such as ascorbic, citric, and acetic acids occurs due to donor–acceptor interactions between the amino groups of chitosan and the acid residues of the corresponding acids. The remaining absorption bands in the IR spectra of chitosan nanoacetate correspond to those of the initial chitosan. The obtained results are shown in Figure 6.

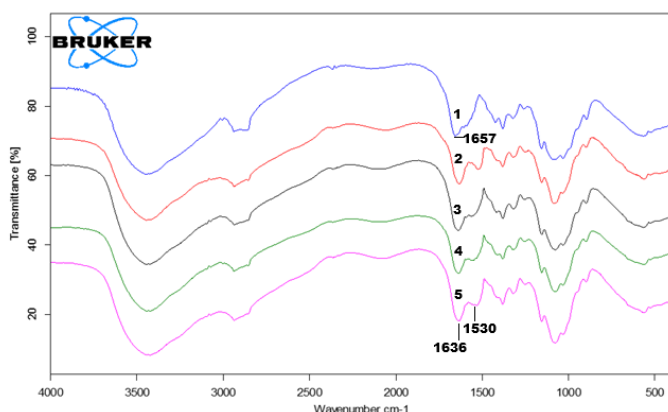


**Figure 6.** IR spectra of the samples: 1. Initial CS; 2. CS:CH<sub>3</sub>COOH at a ratio of 1:1; 3. CS:CH<sub>3</sub>COOH at a ratio of 4:1; 4. CS:CH<sub>3</sub>COOH at a ratio of 3:1; 5. CS:CH<sub>3</sub>COOH at a ratio of 2:1

X-ray structural analysis was performed on the initial chitosan and its nanoderivatives with acetic acid. During the formation of chitosan nanoacetate, a decrease in the intensity of the reflections in the  $2\theta \approx 10.3^\circ$  region was observed. These reflections are associated with the involvement of C-2 amino groups of chitosan in the formation of the crystalline unit cell [17]. The

reduction in the intensity of these reflections may indicate the formation of chitosan–acetic acid complexes through the  $\text{NH}_2$  groups of the macromolecules (Fig. 7).

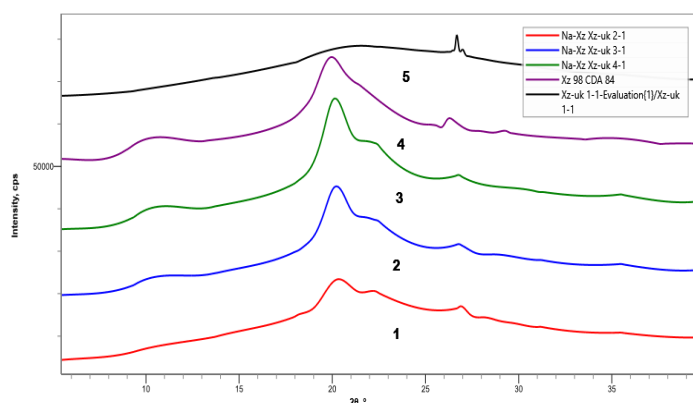


**Figure 7.** XRD results of chitosan nanoacetate at component ratios of 2:1:0.5 (curve 1); 3:1:0.5 (curve 2); 4:1:0.5 (curve 3); initial chitosan (curve 4); and 1:1:0.5 (curve 5).

The obtained results confirm that during the formation of chitosan nanoacetate, no change in the crystal system occurs compared to that of the initial chitosan; that is, the monoclinic crystal system is preserved, with a variation only in the  $\beta^\circ$  angle of the unit cell (Tables 4–6).

For example, during the formation of chitosan nanoascorbate, a transition from a monoclinic to an orthorhombic crystal system was observed, which may be related to differences in the acidity of the acids.

**Table 4**

*XRD results of chitosan nanoacetate (3:1:0.5)*

$2\theta, ^\circ$	$d, \text{\AA}$	Size, $\text{\AA}$	Height, cps	$\alpha, \gamma=90^\circ, \beta=113,9$ monoclinic crystal system, values of h, k, l
10,5	8,40	36,2	1262	100
20,3	4,39	39,3	11721	002
26,9	3,31	111,0	1285	201

**Table 5**

*XRD results of chitosan nanoacetate (4:1:0.5)*

$2\theta, ^\circ$	$d, \text{\AA}$	Size, $\text{\AA}$	Height, cps	$\alpha, \gamma=90^\circ, \beta=91,3$ monoclinic crystal system, values of h, k, l
10,34	8,32	34,8	1883	001
20,1	4,41	40,3	15471	101
26,6	3,29	124,0	1558	10-2

**Table 6**

*XRD results of initial chitosan*

$2\theta, ^\circ$	$d, \text{\AA}$	Size, $\text{\AA}$	Height, cps	$\alpha, \gamma=90^\circ, \beta=95,0$ monoclinic crystal system, values of h, k, l
10,3	8,54	29,6	2518	001
19,7	4,46	25,9	10448	10-1
26,6	3,39	135,0	1418	10-2
35,8	2,52	43,0	674	10-3
40,3	2,23	21,6	458	111











For the study, Petri dishes were first prepared with artificial Czapek nutrient medium based on agar-agar, which is optimal for pathogenic fungi [18]. The fungal culture was then evenly spread over the solid agar medium using a spatula. Circular cuts were made in the center of each culture

dish, and 0.2 mL of chitosan nanoderivative solution with acetic acid was added to each dish [19–20]. Pure cultures of *Fusarium oxysporum* were obtained from the collection of the Institute of Microbiology of the Academy of Sciences of the Republic of Uzbekistan and incubated in a thermostat at 25 °C. The experiments were performed in triplicate. According to the established method, the zones of inhibition caused by the samples were measured over a period of 48 hours [21].

To compare the antimicrobial properties of chitosan nanoacetate, the inhibition zone of *Fusarium oxysporum* growth was determined in Petri dishes cultivated on solidified agar medium for 48 and 72 hours in an incubator at 25 °C. The experiments were carried out in duplicate. The obtained results are presented in Table 7.

Table 7

*Effect of chitosan nanoacetate (CSNA) on the inhibition of Fusarium oxysporum growth*

№	Solutions	Inhibition zone, mm		$\Delta d$ , mm
		48 hours	72 hours	
1	Initial chitosan	 28	 12	20±1
2	Acetic acid	 35	 10	22±5
3	CSNA 4:1 -0,1%	 33	 25	29±2
4	CSNA 3:1 -0,1%	 30	 20	25±2
5	CSNA 2:1 0,1 %	 30	 15	22±2

The obtained results show that the growth and development of fungi of the genus *Fusarium oxysporum*, cultivated on agar medium for 48 hours, were not observed around the mycelium cut. All samples demonstrated antimicrobial properties. Moreover, after 72 hours, active mycelial growth was recorded; however, when using a 0.1% solution of chitosan nanoacetate (component ratio 4:1), a pronounced zone of growth inhibition was noted.

Thus, the structural characteristics of the initial components and chitosan nanoderivatives with acetic acid were studied using various physical and physicochemical methods. It was established that in the IR-spectra of chitosan nanoparticles with organic and inorganic acids, new absorption bands appear in the region of 1510–1530 cm<sup>-1</sup>, corresponding to the formation of donor-acceptor bonds due to the interaction of chitosan amino groups with the acidic residues of the acids. The particle sizes of the chitosan nanoderivatives were determined, and it was shown that with an increase in the chitosan content in the system, the particle sizes increase from 100 nm to 400–500 nm, respectively.

## REFERENCES

- [1]. Malinkina O.N., Provozina A.A., Shipovskaya A.B. Otsenka khimicheskogo vzaimodeystviya gidrokhlorida khitozana s askorbinovoy kislotoi metodami IK- i YaMR-spektroskopii. *Izvestie Saratovskogo universiteta Ser. Khimiya. Biologiya. Ekologiya*. 2014. T. 14, vyp. 3. S. 20–24.
- [2]. Pirniyazov K.K., Anvarova G.K., Rashidova S.Sh. Vliyaniye usloviy sinteza na kompleksoobrazovanie khitozana s askorbinovoy kislotoi. *Izvestiya Ufimskogo nauchnogo tsentra RAN*. 2018. № 3(2). S. 72–74. [https://doi: 10.31040/2222-8349-2018-2-3-72-74](https://doi.org/10.31040/2222-8349-2018-2-3-72-74)
- [3]. Pirniyazov K.K., Milusheva R.Yu., and Rashidova S.Sh. Production and biological activity of chitosan nanoascorbate. *INEOS OPEN*. 2023. Vol. 6(6), pp. 156–162. [https://doi: 10.32931/io2326r](https://doi.org/10.32931/io2326r)
- [4]. Shipovskaya A.B., Fomina V.I., Kireev M.N., Kazakova E.S., Kasyan I.A. Biologicheskaya aktivnost oligomerov khitozana. *Izvestiya Saratovskogo universiteta*. 2008. T. 8. Ser. Khimiya. S. 46–49.
- [5]. Makau S.M., Moumni M., Landi L., Pirozzi D., Sannino F., Romanazzi G. In Vitro Evaluation of Chitosan Hydrochloride and COS (Chito-Oligosaccharides)-OGA (Oligo-Galacturonides) on Phytopathogenic Fungi and *Escherichia coli*. *Horticulturae*. 2023. 9, pp. 1275. <https://doi.org/10.3390/horticulturae9121275>
- [6]. Francesconi S., Steiner B., Buerstmayr H., Lemmens M., Sulyok M., and Balestra G.M. Chitosan Hydrochloride Decreases *Fusarium graminearum* Growth and Virulence and Boosts Growth, Development and Systemic Acquired Resistance in Two Durum Wheat Genotypes. *Molecules*. 2020. Vol. 25, pp. 4752; [https://doi:10.3390/molecules25204752](https://doi.org/10.3390/molecules25204752)
- [7]. Žabka M., Pavela R. The Dominance of Chitosan Hydrochloride over Modern Natural Agents or Basic Substances in Efficacy against *Phytophthora infestans*, and Its Safety for the Non-Target Model Species *Eisenia fetida*. *Horticulturae*. 2021. Vol. 7(10), pp. 366. <https://doi.org/10.3390/horticulturae7100366>
- [8]. Zabka M., Pavela R. Effectiveness of Environmentally Safe Food Additives and Food Supplements in an in Vitro Growth Inhibition of Significant *Fusarium*, *Aspergillus* and *Penicillium* species. *Plant Prot. Sci*. 2018. Vol. 54, 163–173. [https://doi:10.17221/86/2017-PPS](https://doi.org/10.17221/86/2017-PPS)
- [9]. Whisson S.C., Boevink P.C., Wang S.M., Birch P.R.J. The cell biology of late blight disease. *Curr. Opin. Microbiol*. 2016. Vol. 34, 127–135. [https://doi: 10.1016/j.mib.2016.09.002](https://doi.org/10.1016/j.mib.2016.09.002).
- [10]. Savory A.I.M., Grenville-Briggs L.J., Wawra S., van West P., Davidson F.A. Auto-aggregation in zoospores of *Phytophthora infestans*: The cooperative roles of bioconvection and chemotaxis. *J.R. Soc. Interface*. 2014. Vol. 11, 20140017. [https://doi: 10.1098/rsif.2014.0017](https://doi.org/10.1098/rsif.2014.0017)
- [11]. Zabka M., Pavela R., Prokinova E. Antifungal activity and chemical composition of twenty essential oils against significant indoor and outdoor toxigenic and aeroallergenic fungi. *Chemosphere*. 2014. Vol. 112, pp. 443–448. <https://doi.org/10.1016/j.chemosphere.2014.05.014>
- [12]. Inesa V. Blagodatskikh, Sergey N. Kulikov, Oxana V. Vyshivannaya, Evgeniya A. Bezrodnykh and Vladimir E. Tikhonov N-Reacetylated Oligochitosan: pH Dependence of Self-Assembly Properties and Antibacterial Activity. *Biomacromolecules*. 2017. 18(5), pp. 1491–1498. [https://doi: 10.1021/acs.biomac.7b00039](https://doi.org/10.1021/acs.biomac.7b00039)
- [13]. Kulikova S., Tikhonov V., Blagodatskikh I., Bezrodnykh E., Lopatin S., Khairullin R., Philippova Y., Abramchuk S. Molecular weight and pH aspects of the efficacy of oligochitosan against methicillin-resistant *Staphylococcus aureus* (MRSA). *Carbohydr. Polym*. 2012. 87(1), pp. 545–550. [https://doi: 10.1016/j.carbpol.2011.08.017](https://doi.org/10.1016/j.carbpol.2011.08.017).
- [14]. Tanigawa J., Miyoshi N., Sakurai K. Characterization of chitosan/citrate and chitosan/acetate films and applications for wound healing. *Journal of Applied Polymer Science*. 2008. Vol. 110 (1), pp. 608–615. [https://doi:10.1002/app.28688](https://doi.org/10.1002/app.28688)
- [15]. Jubran G. Jabbar Almukhtar and Faiq F. Karam. Preparation characterization and application of Chitosan nanoparticles as drug carrier. *J. Phys.: Conf. Ser*. 2020. pp. 1664 012071. [https://doi:10.1088/1742-6596/1664/1/012071](https://doi.org/10.1088/1742-6596/1664/1/012071)
- [16]. Sodium Acetate Coated Tenofovir-Loaded Chitosan Nanoparticles for Improved Physico-Chemical Properties. *Pharm Res*. 2016. Vol. 33(2), pp. 367–383. [https://doi:10.1007/s11095-015-1795-y](https://doi.org/10.1007/s11095-015-1795-y)

- [17]. Fikry M. Reicha, Ayman S. Shebl, Faried A. Badria and Ahmed A. EL-Asmy. Electrochemical synthesis, characterization and biological activity of chitosan metal complexes. International Journal of Basic and Applied Chemical Sciences. 2012. Vol. 2 (1). pp. 7-22. <http://www.cibtech.org/jcs.htm>
- [18]. Petersen J., McLaughlin S. Laboratory Exercises in Microbiology: Discovering the Unseen erring the Unseen World Through Hands-On Investigation. CUNY Academic Works. 2016. pp. 85-99. [https://academicworks.cuny.edu/qb\\_oers/16](https://academicworks.cuny.edu/qb_oers/16)
- [19]. Abdel-Aliem H.A., Gibriel A.Y., Rasmy N.M.H., Sahab A.F., El-Nekeety A.A., Abdel-Wahhab1 M.A. Antifungal efficacy of chitosan nanoparticles against phytopathogenic fungi and inhibition of zearalenone production by Fusarium graminearum. Com. Sci., Bom Jesus. 2019. Vol. 10, № 3, pp. 338-345. <https://doi:10.14295/CS.v10i3.1899>
- [20]. Guarnieri A., Triunfo M., Scieuzo C. et al. Antimicrobial properties of chitosan from different developmental stages of the bioconverter insect *Hermetia illucens*. Sci Rep. 2022. Vol. 12, pp. 8084. <https://doi.org/10.1038/s41598-022-12150-3>
- [21]. Kumar P.A. Bacterial Resistance to Antimicrobial Agents and Microbiological Quality among *Escherichia coli* Isolated from Dry Fishes in Southeast Coast of India. Roum. Biotechnol. Lett. 2008. Vol. 13, No. 6, pp. 3984-3989. <https://www.researchgate.net/publication/228681375>